Electronic Supplementary Material (ESI) for CrystEngComm.

Supporting Information:

Towards new cesium containing manganese vanadates via a precursor method

Yan-Min Zou,[a,b] Xiao-Yun Lan,[a,b] Wen Ma,[b] Jian-Ce Jin,[b] Hai-Yan Sun,[b] Ji-Long Li,[b] Mei-Ling Feng,[b,*] and Xiao-Ying Huang [b,*]

[a] *College of Chemistry, Fuzhou University, Fuzhou 350116, Fujian, China*

Email: xyhuang@fjirsm.ac.cn; fml@fjirsm.ac.cn

[b]*State Key Laboratory of Structural Chemistry, Fujian Institute of Research on the Structure of Matter, Chinese Academy of Sciences, Fuzhou, Fujian 350002, China.*

Table S1. List of synthetic method and structural dimensionality (D) for selected manganese vanadates.

Formula	Synthesis	D	Ref.
$LiMnVO_4$	Solid-state reaction, 600 °C	3D	1
$NaMnVO_4$	Solid-state reaction, 600 °C	3D	2
$KMnVO_4$	Solid-state reaction, 950 °C	3D	3
$RbMnVO_4$	Solid-state reaction, 650 °C	3D	4
$Na_3MnV_2O_{7.5}$	Solid-state reaction, 950 °C	3D	5
$K_2MnV_2O_7$	Solid-state reaction, 550 °C	2D	6
$Rb_2MnV_2O_7$	Solid-state reaction, 700 °C	2D	6
$KMn_2V_3O_{10}$	Hydrothermal reaction, 180 °C	3D	7
$Li_2Mn(VO_3)_4(H_2O)_2$	Hydrothermal reaction, 110 °C	3D	8
$K_2Mn(VO_3)_4$	Hydrothermal reaction, 180 °C	3D	9
$NaMn_3V_4O_{12}$	Solid-state reaction, 950 °C	3D	10
$NaMn_4(VO_4)_3$	Solid-state reaction, 900 °C	3D	11
$Cs_3Mn_3V_4O_{16}$	Solid-state reaction, 420 °C	2D	12

References

1. M. Sato, S. Kano, S. Tamaki, M. Misawa, Y. Shirakawa and M. Ohashi, *J. Mater. Chem.*, 1996, **6**, 1191-1194.
2. H. Ben Yahia, E. Gaudin, K. Boulahya, J. Darriet, W. J. Son and M. H. Whangbo, *Inorg. Chem.*, 2010, **49**, 8578-8582.
3. H. Ben Yahia, E. Gaudin, C. Lee, M. H. Whangbo and J. Darriett, *Chem. Mater.*, 2007, **19**, 5563-5569.
4. H. Ben Yahia, E. Gaudin and J. Darriet, *J. Solid. State. Chem.*, 2008, **181**, 3103-3109.
5. H. Ben Yahia, E. Gaudin, K. Boulahya and J. Darriet, *Solid State Sci.*, 2011, **13**, 1235-1241.
6. H. Ben Yahia, E. Gaudin and J. Darriet, *Z. Naturforsch. B.*, 2007, **62**, 873-880.
7. O. Yakubovich, L. Shvanskaya, Z. Pchelkina, O. Dimitrova, A. Volkov, O. Volkova and A. Vasiliev, *Acta Crystallogr. B.*, 2018, **74**, 97-103.
8. V. Legagneur, *Solid State Ionics*, 2000, **133**, 161-170.
9. J. H. Liao, C. Sigala, D. Guyomard and Y. Piffard, *Acta Crystallogr. C*, 1996, **52**, 283-284.
10. S. Zhang, T. Saito, M. Mizumaki, W. T. Chen, T. Tohyama and Y. Shimakawa, *J. Am. Chem. Soc.*, 2013, **135**, 6056-6060.
11. O. Clemens, R. Haberkorn, M. Springborg and H. P. Beck, *J. Solid. State. Chem.*, 2012, **194**, 409-415.
12. Y. Lepage and P. Strobel, *Inorg. Chem.*, 1982, **21**, 620-623.

Yield calculation method

The yield of synthesis is calculated based on the following equation based on vanadium.

$$\text{yield } \% = \textbf{Error!} \cdot \textbf{Error!} \times 100\%$$

where F.W. (R) is the formula weight of the reagent containing metal, F.W. (P) is the formula weight of the product containing metal, M (R) is the weight (in grams) of the reagent, and M (P) is the weight (in grams) of the product.

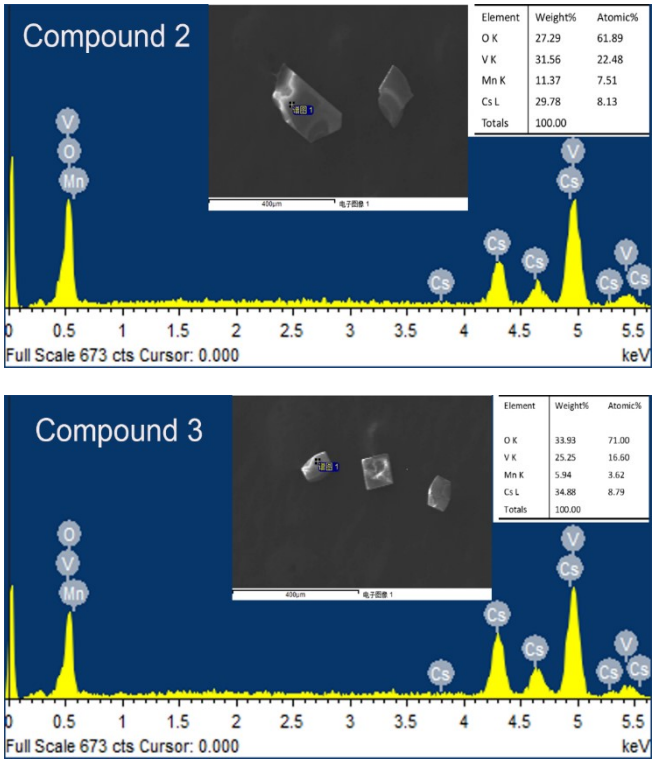

Figure S1. EDS spectra for **2** and **3** displaying the elemental compositions in both weight percentage and atomic percentage. Inset is the EDS image; the magnification is 400 μm, and the area of material is only one point on the face.

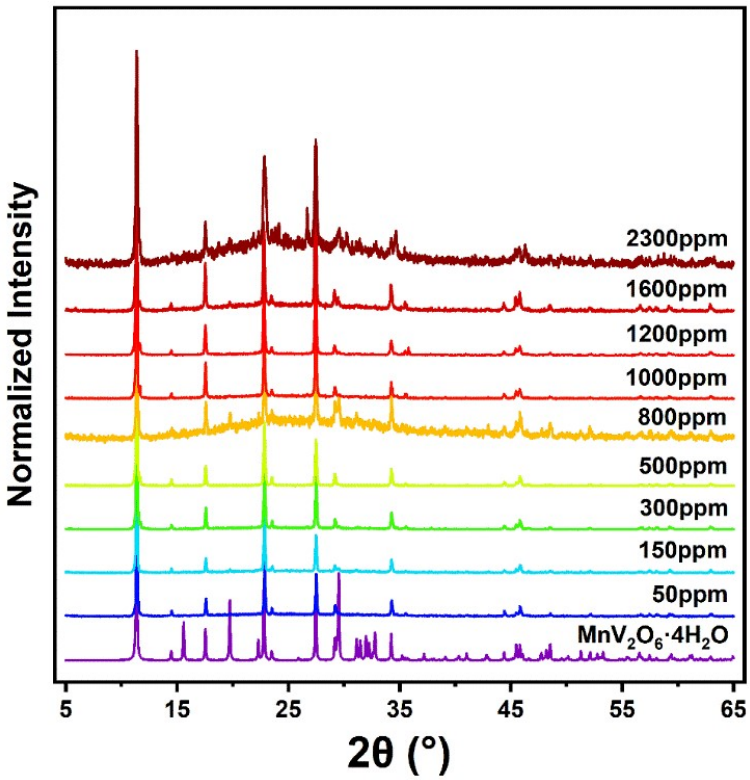

Figure S2. Comparison of the simulated PXRD pattern of $MnV_2O_6 \cdot 4H_2O$ with the experimental ones for the samples generated by immersing **1** in the Cs^+ solutions with varied concentrations of 50-2300 ppm.

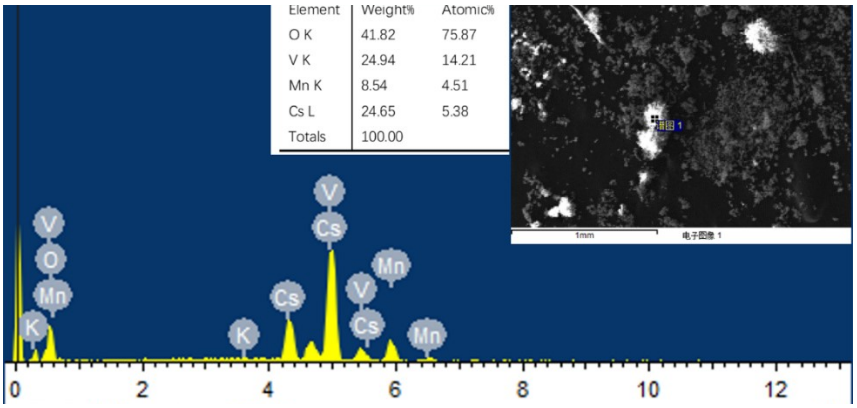

Figure S3. EDS spectrum for the unknown phase obtained in the Cs^+ solutions with varied concentrations of 2500-4000 ppm, displaying elemental composition in weight and atomic percentage. Inset is the EDS image; the magnification is 1 mm, and the area of material is only one point on the face.

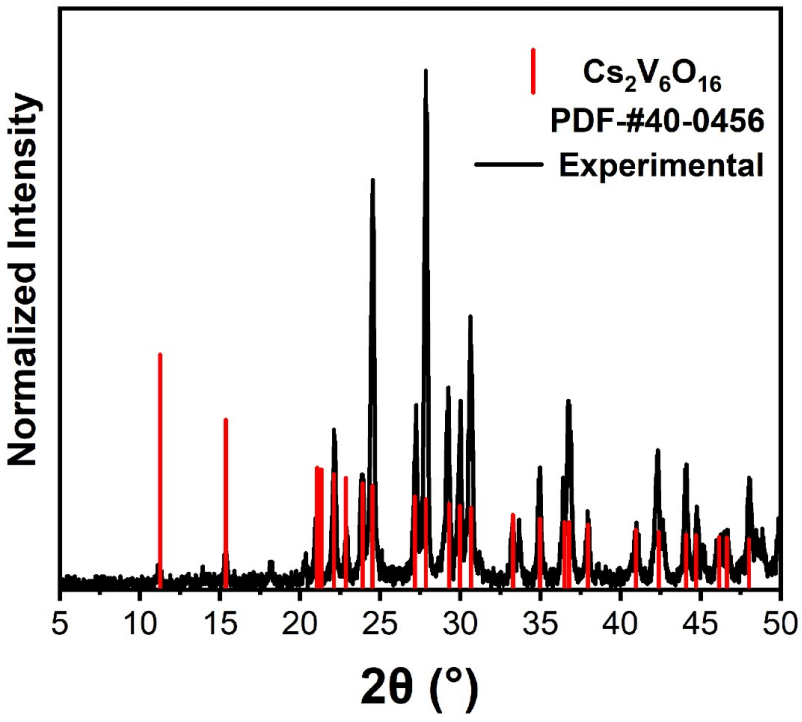

Figure S4. PXRD pattern of the brown powder compared with that from the standard PDF card of $Cs_2V_6O_{16}$.

X-ray crystallography

All non-hydrogen atoms were refined anisotropically. The Cs, Mn and lattice water molecules are highly disordered in compound **3**. Initially their site occupancies were refined and finally fixed to make the crystal electrically neutral and their atomic displacements reasonable. The Cs(3) atoms and O(1W) in **3** were co-occupied, and refined with restraints of EADP and EXYZ.

Table S2. Crystallographic data of **$K_2Mn(VO_3)_4$ (1)**.

Compound	**1**
Empirical formula	$K_2MnO_{12}V_4$
Formula weight	528.90
Crystal system	Monoclinic
Space group	$P2_1/n$
a/Å	8.1777(5)
b/Å	9.1912(4)
c/Å	8.6195(5)
β/°	109.568(6)
V/Å^3	610.45(6)
Z	2
T/K	100 K
λ/Å	0.71073
F(000)	502
ρ_{calcd}/g cm^{-3}	2.877
μ/mm^{-1}	4.688
Measured refls.	13252
Independent refls.	1591
No. of parameters	89
R_{int}	0.0438
R_1 (I> 2σ(I))[a]	0.0397
$wR(F^2)$ (I> 2σ(I))[b]	0.1011
GOF	1.275

[a] $R_1 = \sum \| F_o \| - | F_c \| / \sum | F_o |$, [b] $wR_2 = [\sum w(F_o^2 - F_c^2)^2 / \sum w(F_o^2)^2]^{1/2}$.

Table S3. Selected bond distances (Å) and angles (°) for **1**

Distances		Angles	
Mn(1)-O(4)#1	2.113(3)	O(4)#1-Mn(1)-O(4)#2	180.00(19)
Mn(1)-O(4)#2	2.113(3)	O(4)#1-Mn(1)-O(3)#3	89.28(12)
Mn(1)-O(3)#3	2.125(3)	O(4)#2-Mn(1)-O(3)#3	90.72(12)
Mn(1)-O(3)	2.126(3)	O(4)#1-Mn(1)-O(3)	90.72(12)
Mn(1)-O(5)	2.158(3)	O(4)#2-Mn(1)-O(3)	89.28(12)
Mn(1)-O(5)#3	2.158(3)	O(3)#3-Mn(1)-O(3)	180
V(1)-O(4)	1.648(3)	O(4)#1-Mn(1)-O(5)	90.91(13)
V(1)-O(3)	1.658(3)	O(4)#2-Mn(1)-O(5)	89.09(13)
V(1)-O(2)	1.777(3)	O(3)#3-Mn(1)-O(5)	90.47(12)
V(1)-O(1)	1.787(3)	O(3)-Mn(1)-O(5)	89.53(12)
V(2)-O(6)	1.624(4)	O(4)#1-Mn(1)-O(5)#3	89.09(13)
V(2)-O(5)	1.663(3)	O(4)#2-Mn(1)-O(5)#3	90.91(13)
		O(3)#3-Mn(1)-O(5)#3	89.53(12)
		O(3)-Mn(1)-O(5)#3	90.47(12)
		O(5)-Mn(1)-O(5)#3	180.0
		O(4)-V(1)-O(3)	106.06(17)
		O(4)-V(1)-O(2)	111.65(17)
		O(3)-V(1)-O(2)	109.50(16)
		O(4)-V(1)-O(1)	113.25(16)
		O(3)-V(1)-O(1)	108.73(16)
		O(2)-V(1)-O(1)	107.60(16)
		O(6)-V(2)-O(5)	109.94(18)
		O(6)-V(2)-O(2)#10	111.12(17)
		O(5)-V(2)-O(2)#10	107.71(16)
		O(6)-V(2)-O(1)#7	106.47(17)
		O(5)-V(2)-O(1)#7	108.75(16)
		O(2)#10-V(2)-O(1)#7	112.82(16)
		V(1)-O(1)-V(2)#7	141.81(19)
		V(1)-O(2)-V(2)#6	163.0(2)
		V(1)-O(3)-Mn(1)	149.7(2)
		V(1)-O(4)-Mn(1)#11	158.1(2)

Symmetry transformations used to generate equivalent atoms: #1 *x*-1/2,-*y*+1/2,*z*-1/2; #2 -*x*+1/2,*y*-1/2,-*z*+1/2; #3 -*x*,-*y*,-*z*; #4 *x*+1/2,-*y*-1/2,*z*+1/2; #5 -*x*-1/2,*y*+1/2,-*z*-1/2; #6 -*x*-1/2,*y*+1/2,-*z*+1/2; #7 -*x*,-*y*,-*z*+1; #8 -*x*-1,-*y*,-*z*; #9 *x*-1/2,-*y*-1/2,*z*-1/2; #10 -*x*-1/2,*y*-1/2,-*z*+1/2;#11 -*x*+1/2,*y*+1/2,-*z*+1/2.

.

Table S4. Selected bond distances (Å) and angles (°) for **2** and **3**

(2)		**(3)**	
Mn(1)-O(4)#1	2.1326(1)	Mn(3)-O(5)#1	2.134(10)
Mn(1)-O(4)#2	2.1326(1)	Mn(3)-O(5)	2.134(10)
Mn(1)-O(5)	2.133(2)	Mn(3)-O(2)	2.207(2)
Mn(1)-O(5)#3	2.133(2)	Mn(3)-O(2)#2	2.207(2)
Mn(1)-O(2)#4	2.1678(1)	Mn(3)-O(2)#1	2.207(2)
Mn(1)-O(2)#5	2.1678(1)	Mn(3)-O(2)#3	2.207(2)
V(1)-O(4)	1.6481(1)	O(3)-Mn(1)#6	2.281(3)
V(1)-O(2)	1.6556(1)	O(3)-Mn(1)	2.323(3)
V(1)-O(1)	1.7766(1)	O(3)-Mn(2)	2.335(3)
V(1)-O(3)	1.7827(9)	V(1)-O(3)	1.634(2)
V(2)-O(5)	1.640(2)	V(1)-O(2)	1.644(2)
V(2)-O(5)#7	1.640(2)	V(1)-O(4)	1.7924(1)
V(2)-O(1)#7	1.8065(1)	V(1)-O(1)	1.7958(1)
V(2)-O(1)	1.8065(1)		
O(2)#4-Mn(1)-O(2)#5	180.00(6)	O(5)#1-Mn(3)-O(5)	180
O(5)-Mn(1)-O(5)#3	180	O(5)#1-Mn(3)-O(2)	98.51(6)
O(4)#1-Mn(1)-O(4)#2	180.00(11)	O(5)-Mn(3)-O(2)	81.49(6)
O(4)#1-Mn(1)-O(5)	90.53(8)	O(5)#1-Mn(3)-O(2)#2	98.51(6)
O(4)#2-Mn(1)-O(5)	89.47(8)	O(5)-Mn(3)-O(2)#2	81.49(6)
O(4)#1-Mn(1)-O(5)#3	89.47(8)	O(2)-Mn(3)-O(2)#2	162.99(12)
O(4)#2-Mn(1)-O(5)#3	90.53(8)	O(5)#1-Mn(3)-O(2)#1	81.49(6)
O(4)#1-Mn(1)-O(2)#4	87.41(7)	O(5)-Mn(3)-O(2)#1	98.51(6)
O(4)#2-Mn(1)-O(2)#4	92.59(7)	O(2)-Mn(3)-O(2)#1	86.51(12)
O(5)-Mn(1)-O(2)#4	93.12(8)	O(2)#2-Mn(3)-O(2)#1	96.01(13)
O(5)#3-Mn(1)-O(2)#4	86.88(8)	O(5)#1-Mn(3)-O(2)#3	81.49(6)
O(4)#1-Mn(1)-O(2)#5	92.59(7)	O(5)-Mn(3)-O(2)#3	98.51(6)
O(4)#2-Mn(1)-O(2)#5	87.41(7)	O(2)-Mn(3)-O(2)#3	96.01(13)
O(5)-Mn(1)-O(2)#5	86.88(8)	O(2)#2-Mn(3)-O(2)#3	86.51(12)
O(5)#3-Mn(1)-O(2)#5	93.12(8)	O(2)#1-Mn(3)-O(2)#3	162.99(12)
O(4)-V(1)-O(2)	110.45(10)	O(3)#12-Mn(1)-O(3)#8	88.36(17)
O(4)-V(1)-O(1)	109.45(9)	O(1W)-Mn(1)-O(3)#11	82.96(12)
O(2)-V(1)-O(1)	110.19(9)	O(3)#12-Mn(1)-O(3)#11	91.20(12)
O(4)-V(1)-O(3)	108.44(11)	O(3)#8-Mn(1)-O(3)#11	167.05(19)
O(2)-V(1)-O(3)	110.04(1)	O(3)#12-Mn(1)-O(3)	167.05(19)
O(1)-V(1)-O(3)	108.23(1)	O(3)#8-Mn(1)-O(3)	91.20(12)
O(5)-V(2)-O(5)#7	108.64(1)	O(3)#11-Mn(1)-O(3)	86.34(17)
O(5)-V(2)-O(1)#7	108.26(9)	O(3)#16-Mn(2)-O(3)#8	89.56(9)
O(5)#7-V(2)-O(1)#7	110.04(9)	O(3)#16-Mn(2)-O(3)#18	89.56(9)
O(5)-V(2)-O(1)	110.04(9)	O(3)#8-Mn(2)-O(3)#18	169.9(11)
O(5)#7-V(2)-O(1)	108.26(9)	O(3)#16-Mn(2)-O(3)	169.9(11)
O(1)#7-V(2)-O(1)	111.57(12)	O(3)#8-Mn(2)-O(3)	89.56(9)
V(1)-O(1)-V(2)	132.05(11)	O(3)#18-Mn(2)-O(3)	89.56(9)

V(1)-O(3)-V(1)#10	159.82(17)	O(3)-V(1)-O(2)	108.60(12)
V(1)-O(2)-Mn(1)#11	134.37(10)	O(3)-V(1)-O(4)	108.75(11)
V(1)-O(4)-Mn(1)#8	150.84(12)	O(2)-V(1)-O(4)	110.56(14)
V(2)-O(5)-Mn(1)	143.94(12)	O(3)-V(1)-O(1)	108.36(14)
H(1)-O(1W)-H(1)#10	118(7)	O(2)-V(1)-O(1)	111.79(14)
		O(4)-V(1)-O(1)	108.72(13)
		V(1)#3-O(4)-V(1)	136.6(2)
		V(1)#9-O(1)-V(1)	137.18(19)
		V(1)-O(2)-Mn(3)	132.50(14)
		V(1)-O(3)-Mn(1)#6	140.21(18)
		V(1)-O(3)-Mn(1)	138.85(16)
		V(1)-O(3)-Mn(2)	136.9(5)

Symmetry transformations used to generate equivalent atoms for **2**: #1 *-x*,*-y*+1,*-z*; #2 *x*+1,*y*,*z*; #3 *-x*+1,*-y*+1,*-z*; #4 *x*+1,*-y*+1/2,*-z*; #5 *-x*,*y*+1/2,*z*; #6 *-x*+1,*y*+1/2,*z*; #7 *x*,*-y*+1/2,*-z*; #8 *x*-1,*y*,*z*; #9 *-x*,*y*-1/2,*z*; #10 *x*,*y*,*-z*+1/2; #11 *x*-1,*-y*+1/2,*-z*; #12 *x*+1,*y*,*-z*+1/2; #13 *-x*,*y*-1/2,*-z*+1/2.

Symmetry transformations used to generate equivalent atoms for **3**: #1 *y*+1/2,*x*-1/2,*-z*+1/2; #2 *-x*+1,*-y*,*z*; #3 *-y*+1/2,*-x*+1/2,*-z*+1/2; #4 *-y*+1/2,*-x*+1/2,*z*-1/2; #5 *-x*+1,*-y*,*-z*+1; #6 *y*,*-x*+1,*-z*+1; #7 *x*-1/2,*-y*+1/2,*z*-1/2; #8 *-y*+1,*x*,*z*; #9 *x*,*y*,*-z*; #10 *-x*+1,*-y*,*-z*; #11 *x*,*y*,*-z*+1; #12 *-y*+1,*x*,*-z*+1; #13 *y*+1/2,*x*-1/2,*z*+1/2; #14 *-x*+1,*-y*+1,*-z*; #15 *y*,*-x*+1,*-z*; #16 *-x*+1,*-y*+1,*z*; #17 *-y*+1,*x*,*-z*; #18 *y*,*-x*+1,*z*; #19 *-x*+1,*-y*+1,*-z*+1.

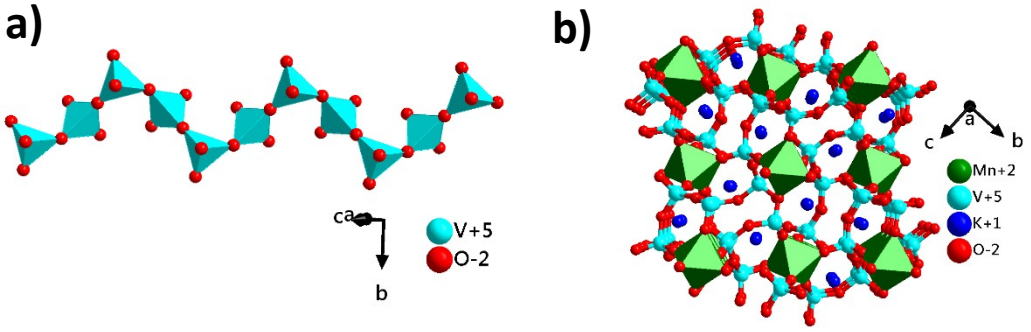

Figure S5. a) The $(VO_3)_n$ chain in **1**. b) The 3D structure of **1** viewed along the *a*-axis.

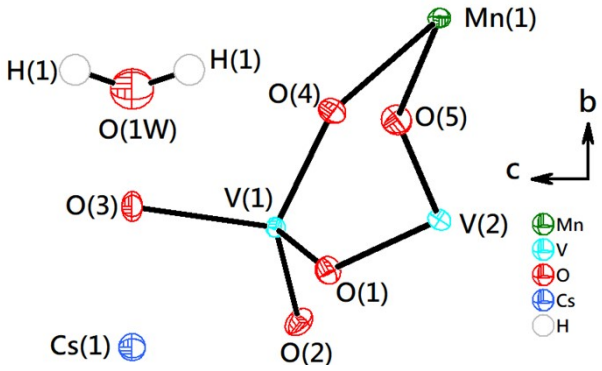

Figure S6. *Ortep* drawing (50% ellipsoid probability) of the asymmetric unit of **2**.

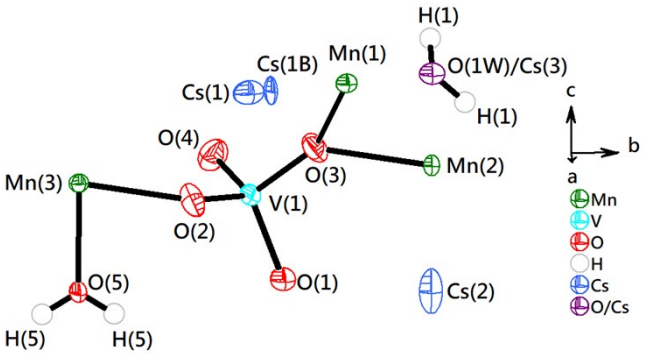

Figure S7. *Ortep* drawing (50% ellipsoid probability) of the asymmetric unit of **3.**

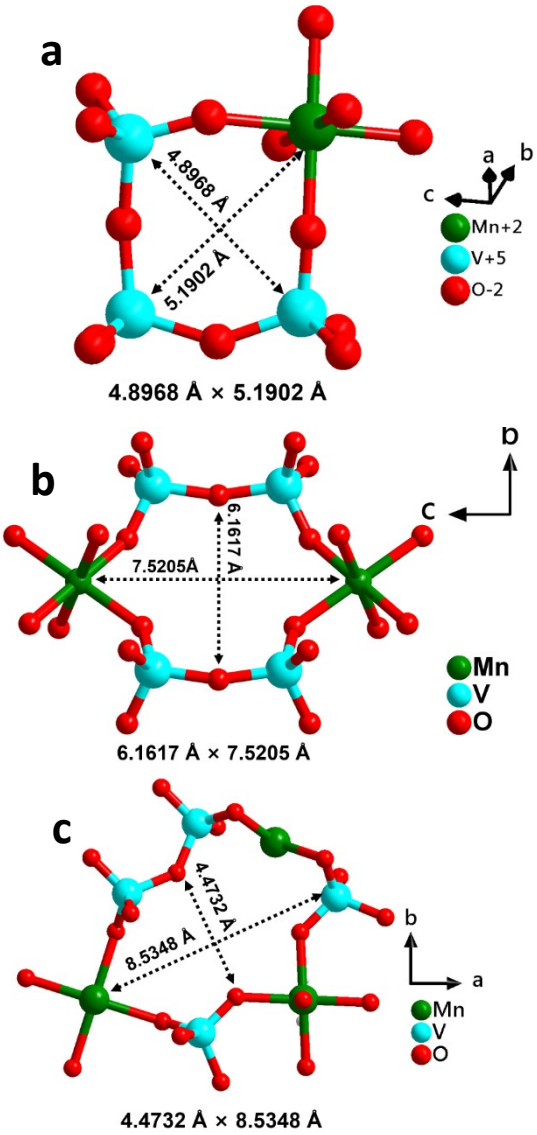

Figure S8. The cross section of channel in **1** (a), **2** (b) and **3** (c).

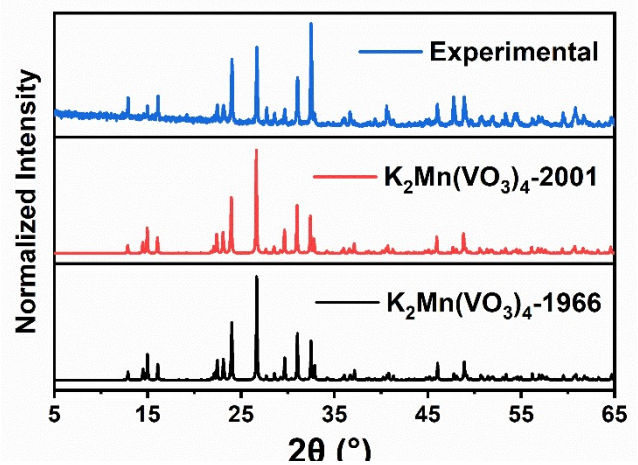

Figure S9. Simulated and experimental PXRD patterns for $K_2Mn(VO_3)_4$.

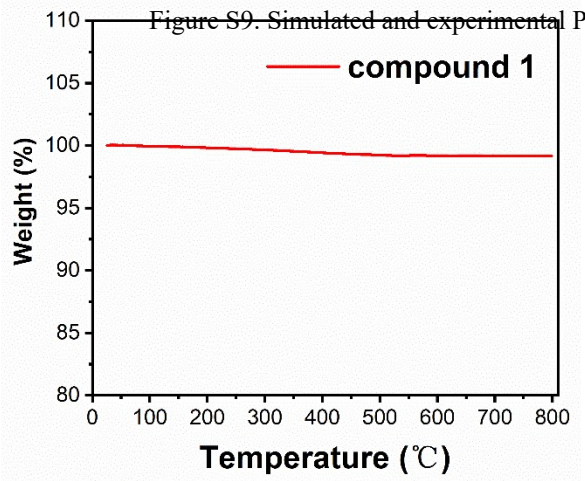

Figure S10. TG curve of **1**.

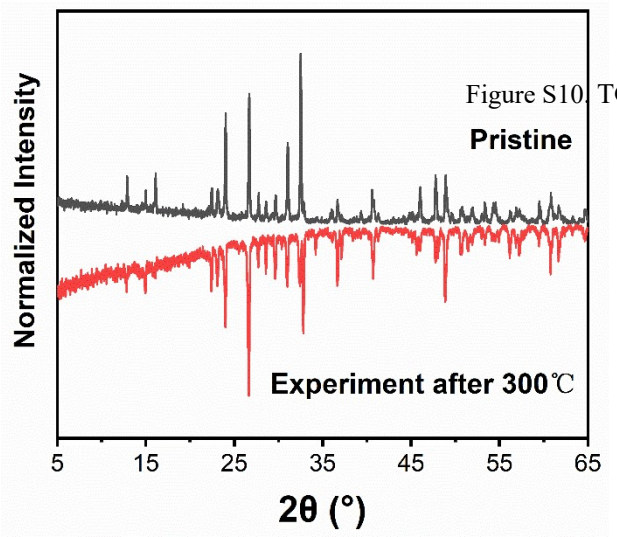

Figure S11. The original PXRD pattern of **1** compared with that of sample after heating to 300 °C.

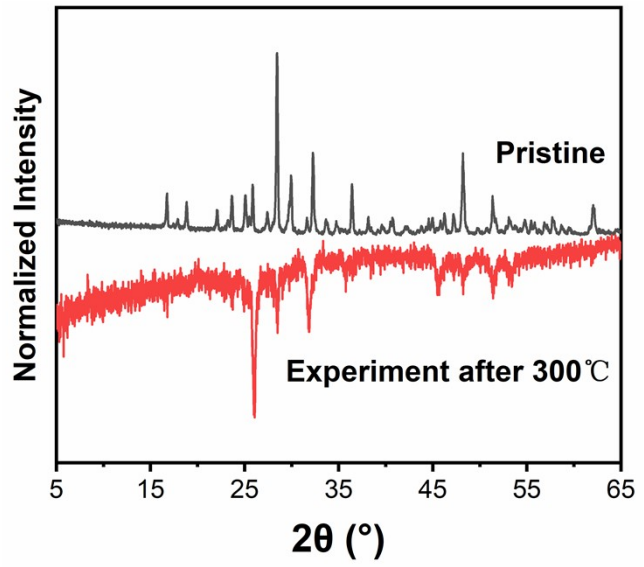

Figure S12. The original PXRD pattern of **2** compared with that of sample after heating to 300 °C.

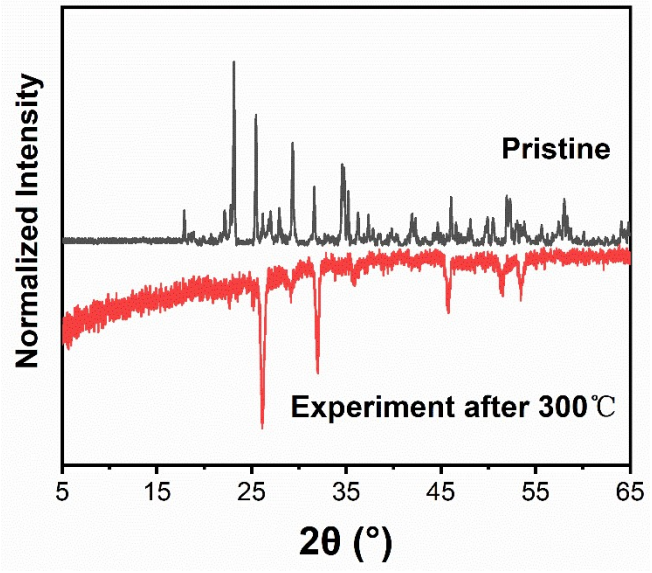

Figure S13. The original PXRD pattern of **3** compared with that of sample after heating to 300 °C.